Measurement of Self-Loop Function and Stability Test for Third-order Sallen-Key Low-Pass Filters

MinhTri Tran, Anna Kuwana, Haruo Kobayashi (Gunma University)

This paper presents a stability test for a third-order Sallen-Key low-pass filter. The self-loop function of this filter is derived based on an alternating current conservation technique. A passive balun transformer is used to measure the phase margin at unity gain of the self-loop function in an implemented circuit. The values of theoretical calculation are verified by the SPICE simulation and practical measurement results. Therefore, our proposed measurement technique is considered for examining the behavior of a linear network.

Keywords: Superposition, Sallen-Key LPF, Phase Margin, Self-loop Function, Alternating Current Conservation.

1. INTRODUCTION

Mathematical models deal with the physical reality of the linear system [1]. Moreover, its transfer function and self-loop function are very important because they give some useful information about stability and help us optimize the entire performance of a system [2]. The most focus of recent researches is by the necessity on the theory that underlies the design, performance analysis and stability test of the various networks [3]. From the view point of the complex function, the operating regions of a high-order system are classified as over-damping, critical damping, and under-damping. As a high-order system operates on the under-damping region, the damped oscillation noise causes ringing and makes the network unstable. Ringing or overshoot voltage occurs in both passive and active systems. In other words, it occurs in both feedback and non-feedback systems [4].

To do the stability test of a feedback network, the conventional root locus, Nyquist plot, and Nichols plot techniques all make use of the complex plane [5]. In the root locus method, if a system has poles that are in the right half plane, it will be unstable. Various stabilization conditions were derived using the Nyquist stability criterion. In most cases, Nyquist and Nichols theorems are used in theoretical analysis for feedback systems [6]. Nyquist's theorem shows that the polar plot of loop gain must not encircle the point (−1, 0), where the direction of the encirclement is clockwise [7]. There are some limitations in the conventional methods:

- The relationship between the transfer function and the loop gain in a general system is not clarified well. The loop gain is used only in the flow graph signal of a feedback system. The phase margin at unity gain of the loop gain is not analyzed mathematically well.
- Behaviors of a high-order transfer function in passive and active systems are not studied clearly [8]. In conventional measurement of the loop gain, the theoretical derivation and practical measurement are not well explained.
- Sufficient numerical examples of the phase margin at unity gain of the loop gain are not introduced. Moreover, the relationship between the replica measurement and the Middlebrook's method was not mentioned before. These methods were not applied to the stability test of high-order low-pass filters.

To overcome the limitations of the conventional methods, the measurement of the phase margin at unity gain of the self-loop function is proposed to evaluate the quality of a high-order system. The motivation for this work on measurement of the self-loop function is coming from the high degree of performance capabilities; therefore, the investigation of the phase margin at unity gain of the self-loop function has been the focal point of extensive research work.

In wireless communication systems, high-order active low-pass filters are widely used. Moreover, to reduce the white noise and random noise, the differential architectures are used in many deigns. This paper also introduces a topology of a differential third-order

Sallen-Key low-pass filter.

This paper contains a total of 5 sections. Section 2 presents the basic research background. Section 3 mathematically analyzes a third-order differential Sallen-Key low pass filter in details. Experimental results of measurements of self-loop functions are described in Section 4. The main points of this work are summarized in Section 5.

2. MODELS OF ELECTRONIC SYSTEMS

Passive and active linear networks can be modeled by the transfer functions. When the input source, output signal, and some other sources in the internal dynamics of a network are known, the transfer function is used to examine the behavior of the network. The transfer function H(ω) of a filter is the ratio of the output signal $V_{out}(\omega)$ to the input signal Vin(ω) as a function of the frequency. A general transfer function is rewritten as

$$H(\omega)=\frac{V_{out}(\omega)}{V_{in}(\omega)}=\frac{A(\omega)}{1+L(\omega)} =\frac{b_0(j\omega)^n+b_1(j\omega)^{n-1}+...+b_{n-1}(j\omega)+b_n}{a_0(j\omega)^n+a_1(j\omega)^{n-1}+...+a_{n-1}(j\omega)+a_n} \quad (1)$$

Here, A(ω) is the numerator function of the transfer function, and L(ω) is the self-loop function in the denominator of the self-loop function. A self-loop function analysis is a very useful tool for linear systems. The phase margin of the self-loop function is directly related to the transient response of a system.

Fig. 1 shows a setup using the alternating current conservation method using a balun transformer to measure the self-loop function [9]. The main idea of this method is that the alternating current is conserved. In other words, at the output node the incident alternating current is equal to the transmitted alternating current. If we inject an alternating current source (or alternating voltage source) at the output node, the self-loop function can be derived by ratio of the incident voltage (V_{inc}) and the transmitted voltage (V_{trans}). Apply the widened superposition principle at V_{inc} and V_{trans} nodes, and then the self-loop function is derived as

$$\frac{V_{inc}}{A(\omega)}=-\frac{L(\omega)}{A(\omega)}V_{trans}\Rightarrow L(\omega)=-\frac{V_{inc}}{V_{trans}} \quad (2)$$

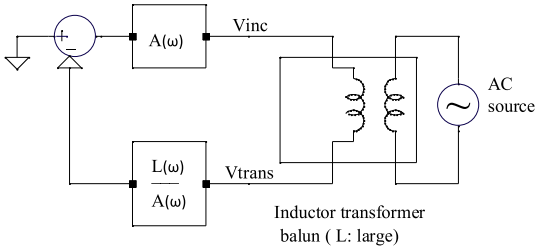

Fig. 1. Derivation of the self-loop function

3. THIRD-ORDER SALLEN-KEY FILTER

3.1. Fully differential two-stage op amp

Fully differential op amp has two input sources and two output signals which are called positive output and negative output. These output voltages are equal, but opposite in polarity referenced to the common-mode operating point of the circuit as shown in Fig. 2.

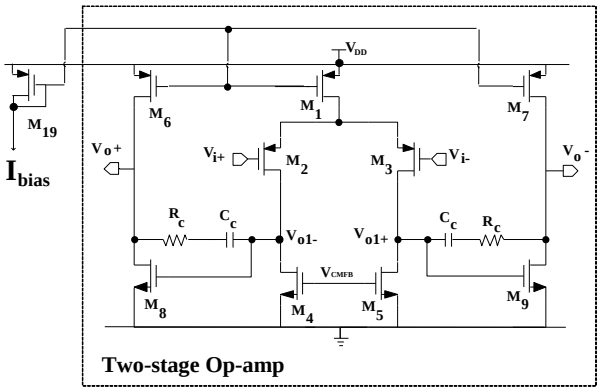

(a) Fully-differential two-stage op amp.

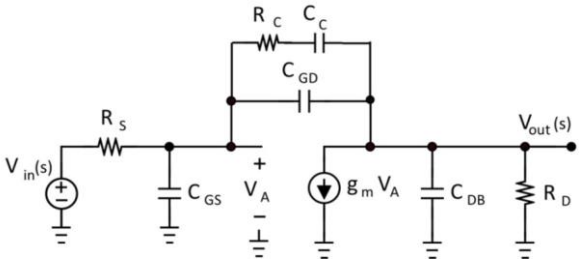

(b) Small signal model of the second-stage.

Fig. 2. Schematic of the fully-differential op amp.

The transfer function and the self-loop function are derived as

$$H(\omega)=\frac{b_0(j\omega)^3+b_1(j\omega)^2+b_2j\omega+b_3}{a_0(j\omega)^4+a_1(j\omega)^3+a_2(j\omega)^2+a_3j\omega+1} \quad (2)$$
$$L(\omega)=a_0(j\omega)^4+a_1(j\omega)^3+a_2(j\omega)^2+a_3j\omega$$

Where, the values of the constant variables are

$$b_0 = R_D\left(R_C C_C\right)^2 C_{GD};\ b_1 = R_D R_C C_C\left(2C_{GD} + C_C - g_m R_C C_C\right)$$
$$b_2 = R_D\left(C_{GD} + C_C - 2g_m R_C C_C\right);\ b_3 = -g_m R_D;$$
$$a_0 = R_D R_S\left(R_C C_C\right)^2\left[\left(C_{GD} + C_{DB}\right)C_{GS} + C_{GD}C_{DB}\right]$$
$$a_1 = R_C C_C\left\{\begin{bmatrix} R_C C_C\begin{bmatrix} R_D\left(C_{GD} + C_{DB}\right) \\ +R_S\left(C_{GS} + C_{GD}\right) + R_S R_D C_{GD} g_m \end{bmatrix} \\ +R_S R_D\left[2\left(C_{GS} + C_{DB}\right)\left(C_{GD} + C_{GS}\right) + C_C C_{GS}\right] \end{bmatrix}\right\}$$
$$a_2 = \left\{\begin{bmatrix} R_C C_C\left[R_C C_C + 2R_D\left(C_{GD} + C_{DB}\right) + C_C\left(R_D + R_S\right)\right] \\ +R_S C_C\left[2R_C\left(C_{GS} + C_{GD}\right) + R_D\left(C_{GS} + C_{DB}\right)\right] \\ +R_S R_D\left[C_{GS}\left(C_{GD} + C_{DB}\right) + C_{GD}C_{DB}\right] \\ +g_m R_S R_D R_C\left(2C_{GD} + C_C\right) \end{bmatrix}\right\} \quad (3)$$
$$a_3 = \left\{\begin{bmatrix} \left(R_C + R_D\right)C_C + R_D\left(C_{GD} + C_{DB}\right) + R_C C_C \\ +R_S\left[\left(C_{GS} + C_{GD} + C_C\right) - g_m R_D\left(C_{GD} + C_C\right)\right] \end{bmatrix}\right\}$$

The transfer function at the second-stage of op amp is a fourth-order complex function. The Miller's capacitor will affect the operating region of the total op amp. Here, the designed gain bandwidth and the DC gain of the fully differential op amp are GBW =10 MHz, Ao = 100000, respectively. The cut-off frequency is designed at 100 Hz. The open-loop function A(ω) and self-loop function L(ω) of the op amp are

$$A(\omega) = \frac{10^5}{1 + j\dfrac{\omega}{200\pi}};\ L(\omega) = j\frac{\omega}{200\pi} = 10^5\frac{V_{in}}{V_{out}} - 1 \quad (4)$$

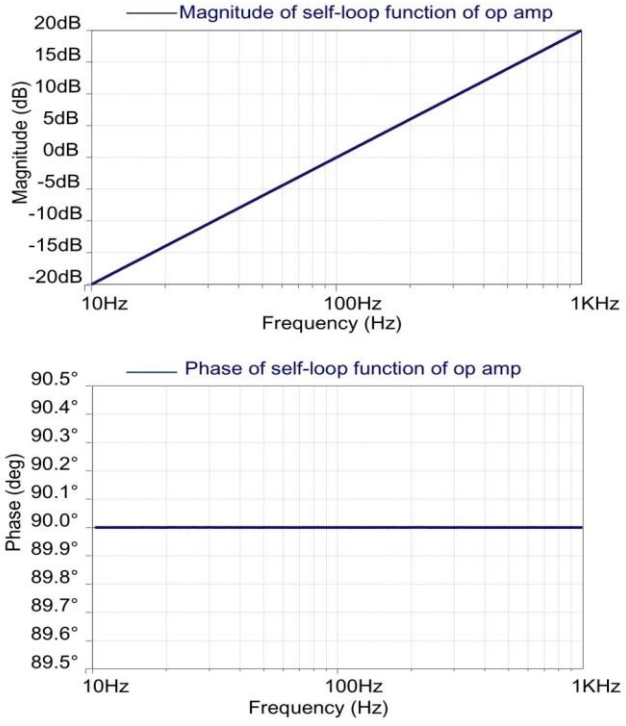

Fig. 3. Bode plots of the self-loop function L(ω).

The frequency responses of the self-loop function of the op amp are shown in Fig. 3. The phase margin at unity gain of the self-loop function is 90-degrees, this op amp is absolutely stable.

3.2. Design of third-order Sallen-key LPF

Differential topology is applied in many active low-pass filters. From a differential low-pass filter, we can design an active complex filter [10]. In this paper, we introduce a differential third-order low-pass filter based on the Sallen-Key's connection. Fig. 4 shows the proposed design of a differential third-order Sallen-Key low-pass filter. The values of passive components are resistors $R_1 = R_2 = R_3 = 10$ kΩ, $R_4 = 100$ Ω, $R_5 = 100$ kΩ, capacitors $C_1 = 350$ pF, $C_2 = 2$ nF, at the cut-off frequency $f_0 = 10$ kHz. Three values of capacitor C_3 (2 nF, 1 nF, and 0.2 nF) are used to examine the behaviors of the differential third-order Sallen-Key low-pass filter.

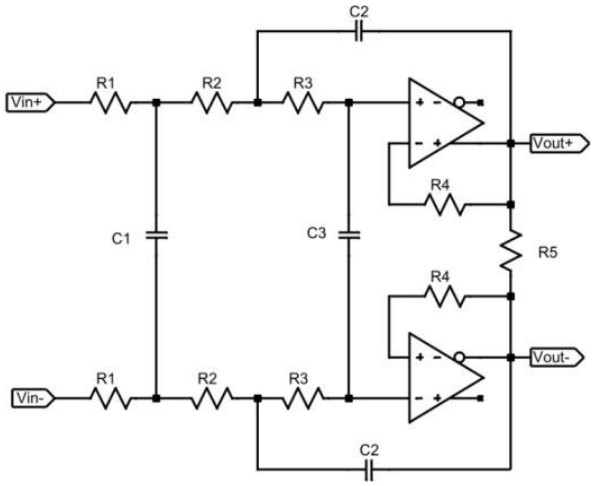

Fig. 4. Schematic of the proposed design.

Its transfer function and self-loop function are

$$H(\omega) = \frac{b_0}{a_0\left(j\omega\right)^3 + a_1\left(j\omega\right)^2 + a_2 j\omega + 1};$$
$$L(\omega) = a_0\left(j\omega\right)^3 + a_1\left(j\omega\right)^2 + a_2 j\omega; \quad (5)$$

Here, the given values of constant variables are

$$b_0 = 1 + \frac{R_4}{R_5};\ a_0 = R_1 C_1 R_2 C_2 R_3 C_3;$$
$$a_1 = R_1 C_1 C_3\left(R_2 + R_3\right) + R_3 C_2 C_3\left(R_1 + R_2\right) - \frac{R_4}{R_5}R_1 C_1 R_2 C_2; \quad (6)$$
$$a_2 = R_1\left(C_1 + C_3\right) + C_3\left(R_2 + R_3\right) - \frac{R_4}{R_5}\left(R_1 + R_2\right)C_2;$$

3.3. Behavior of third-order Sallen-key LPF

The behaviours of the proposed design of a differential third-order Sallen-Key low-pass filter are described in Fig. 5. In case of the under-damping, the overshoot causes extra voltage and makes the system unstable. The Bode plots of the transfer function show that the -3dB bandwidth cannot be applied for high-order transfer function. In case of critical damping, the magnitude of the transfer function at the cut-off frequency is -9 dB, the phase is -135 degrees.

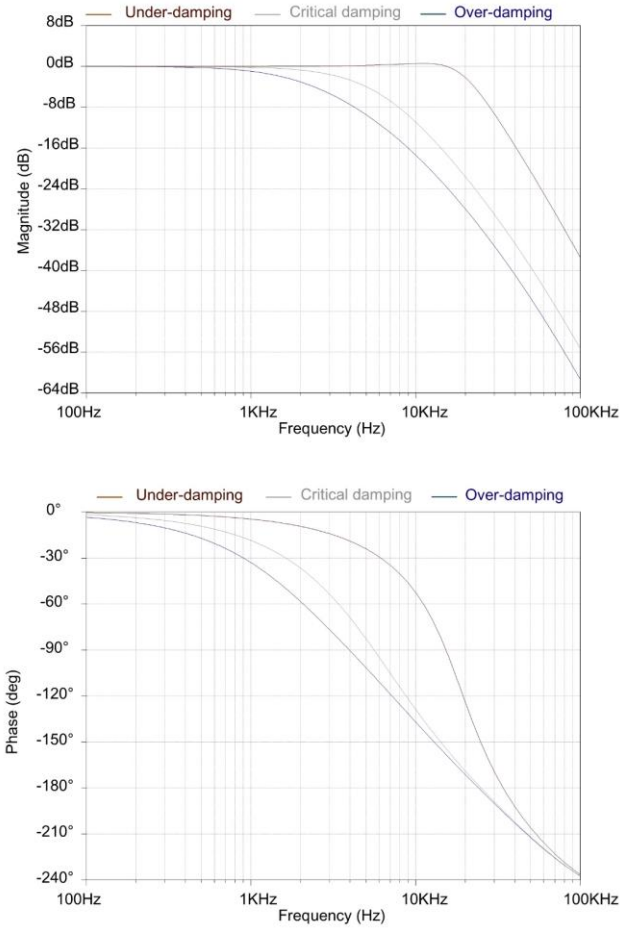

Fig. 5. Bode plots of the transfer function.

3.4. Stability test for third-order Sallen-Key LPF

Two identical balun transformers are used to derive the self-loop function of the third-order differential Sallen-Key low-pass filter as shown in Fig. 6.

The Bode plots of the self-loop function are used to investigate the operating region of the proposed design filter. Fig. 7 shows the phase margin at unity gain of the self-loop function in the frequency domain.

Simulation results of third-order self-loop functions show that the phase margin of the over-damping is 79-degrees, critical damping 72-degrees, and under-damping 60-degrees.

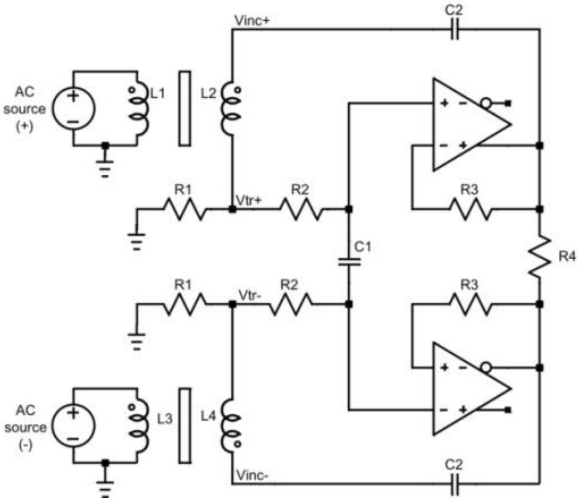

Fig. 6. Schematic of the derivation of the self-loop function.

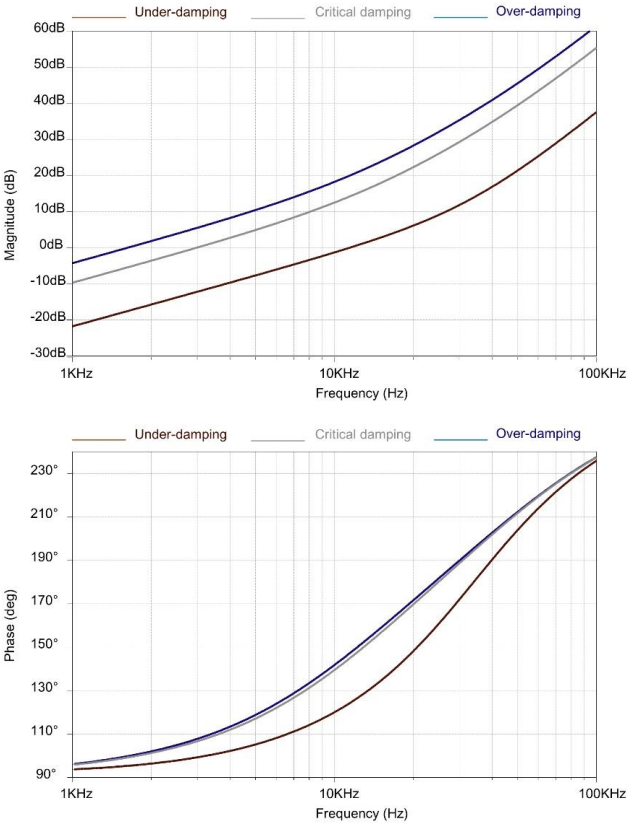

Fig. 7. Bode plots of the self-loop function.

4. EXPERIMENTAL RESULTS

4.1. Implementation of third-order Sallen-Key LPF

Fig. 8 shows the schematic and the implemented circuit of the designed third-order Sallen-Key low-pass filter. A commercial op amp LM358 was used in this implementation.

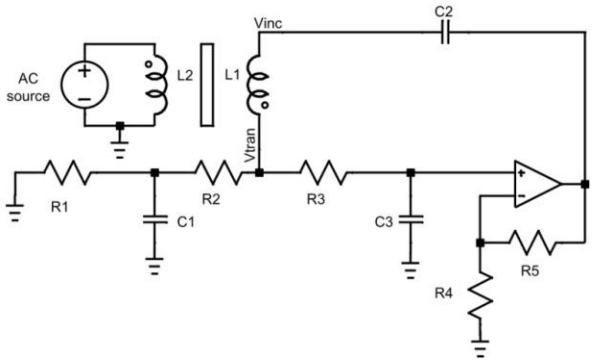

(a) Schematic of the third-order Sallen-Key LPF.

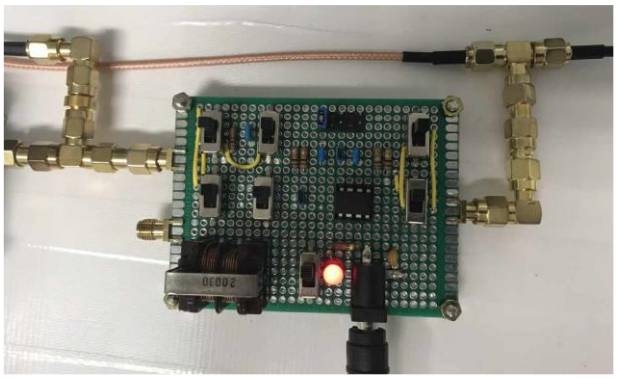

(b) Implemented circuit.

Fig. 8. Design of the third-order Sallen-Key LPF.

The values of passive components are resistors R1 = R2 = R3 = 10 kΩ, R4 = 100 Ω, R5 = 100 kΩ, capacitors C1 = 350 pF, C2 = 2 nF, at the cut-off frequency f0 = 3 kHz. A passive 10 mH balun transformer was used to measure the phase margin at unity gain of the self-loop function.

4.2. Measurement set up

When an active low-pass filter circuit was designed, it is important to know the behavior of the transfer function of the used low-pass filter. Network analyzer, spectrum analyzer, signal generator, oscilloscope, and power supply were used to perform the measurements.

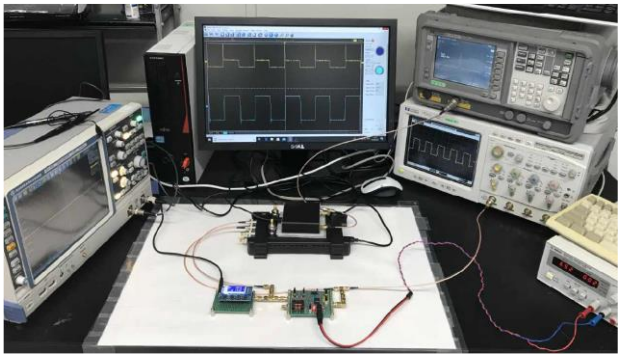

Fig. 9. Measurement set up of implemented circuit.

4.3. Measurement results

Fig. 10 shows the measurement results of the frequency responses of third-order Sallen-Key filters. The cut-off frequency of the implemented third-order Sallen-Key is designed at 3 kHz. In case of the under-damping, the overshoot is very high 2.8 V compared to the desired level 0.5 V. The measured waveforms of the transient responses are plotted in Fig. 11.

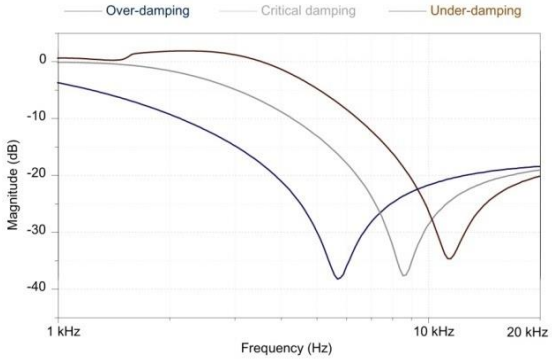

Fig. 10. Measurement results of frequency responses

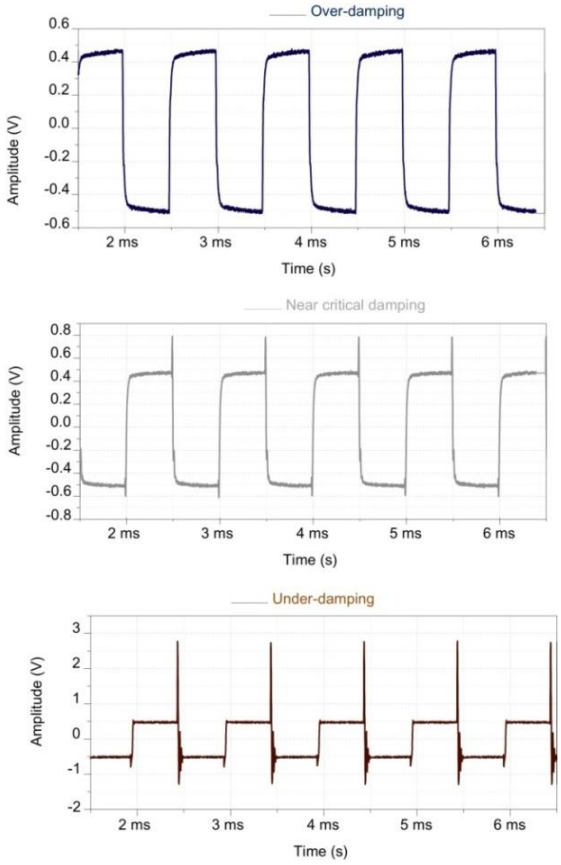

Fig. 11. Measurement of transient responses.

4.4. Phase margin of third-order Sallen-key LPF

The gain margins at unity gain of the self-loop functions are shown in Fig. 12.

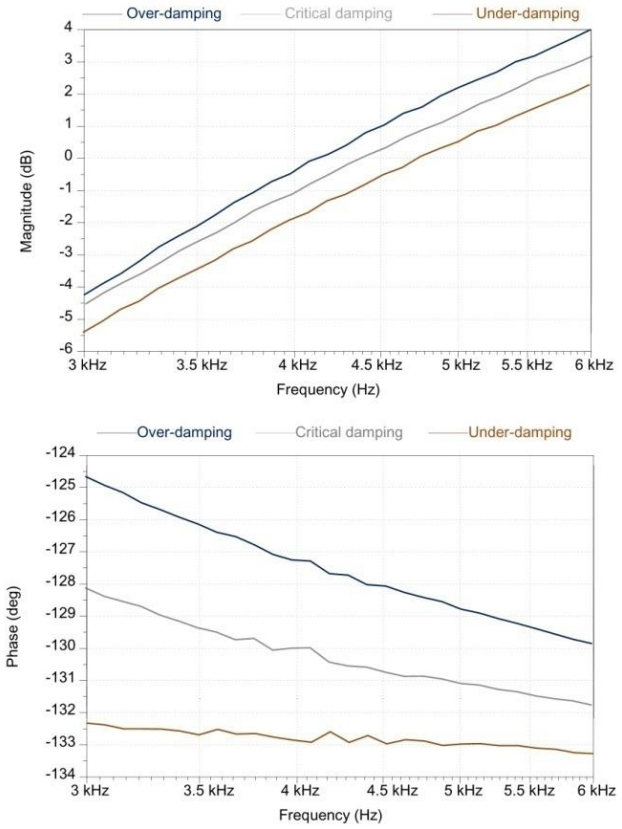

Fig. 12. Measurement results of self-loop functions.

The impedance of the passive balun transformer affects the input impedance of the measurement probes. The measurement results of self-loop functions show that the phase margin of under-damping is 47 degrees. The phase margin of critical damping is 49.5 degrees (still under-damping). The phase margin of case 3 is 52.5 degrees (near critical damping).

5. CONCLUSION

In this paper it has been shown the theoretical analysis of a third-order self-loop function and the measurements of the proposed designs of a third-order Sallen-Key low-pass filter. In order to show the operating regions of single-ended and differential third-order low-pass filters, the transfer function and its self-loop function are determined.

The simulation results were verified by the practical measurements. In the work the stability test is not only analyzed by the numerical examples but also performed by the experimental results of measurements of the designed circuit. In case of a second-order low-pass filter, if its phase margin is smaller than 76.3-degrees, this network is unstable.

The self-loop function of a low-pass filter gives useful information about the relative stability and helps us optimize the closed-loop performance. The self-loop function can be directly calculated based on the widened superposition principle. The alternating current conservation technique can measure the self-loop function of low-pass filters. Compared to the measurement results with mathematical analysis, the properties of self-loop functions are the same.

In future of work, we will investigate the behaviors of high-order complex filters based on the Sallen-Key low-pass connections.

Acknowledgment

Foremost, we would like to express our sincere gratitude to Prof. H. Tanimoto (Kitami Institute of Technology) for continuing supports.

References

(1) H. Kobayashi, N. Kushita, M. Tran, K. Asami, H. San, A. Kuwana "Analog - Mixed-Signal - RF Circuits for Complex Signal Processing", 13th IEEE International Conference on ASIC (ASICON 2019) Chongqing, China, Nov, 2019.

(2) G. F. Franklin, J. D. Powell, A. Emami, Feedback Control of Dynamic Systems, 6th Edition, Prentice-Hall, Boston, 2010.

(3) N. Kumar, V. Mummadi, "Stability Region Based Robust Controller Design for High-gain Boost DC-DC Converter", IEEE Transactions on Industrial Electronics, Feb. 2020.

(4) L. Fan, Z. Miao, "Admittance-Based Stability Analysis: Bode Plots, Nyquist Diagrams or Eigenvalue Analysis", IEEE Transactions on Power Systems, Vol. 35, Issue 4, July 2020.

(5) R. Middlebrook, "Measurement of Loop Gain in Feedback Systems", Int. J. Electronics, Vol 38, No. 4, pp. 485-512, 1975.

(6) P. Wang, S. Feng, P. Liu, N. Jiang, X. Zhang, "Nyquist stability analysis and capacitance selection method of DC current flow controllers for meshed multi-terminal HVDC grids", CSEE Journal of Power and Energy Systems, July 2020, pp. 1-13.

(7) N. Tsukiji, Y. Kobori, H. Kobayashi, "A Study on Loop Gain Measurement Method Using Output Impedance in DC-DC Buck Converter",IEICE Trans. Communications, Vol.E101-B, No.9, pp.1940-1948, Sep. 2018.

(8) J. Wang, G. Adhikari, N. Tsukiji, H. Kobayashi, "Analysis and Design of Operational Amplifier Stability Based on Routh-Hurwitz Stability Criterion", IEEJ Trans. Electronics, Information and Systems, Vol. 138, No. 128, pp.1517-1528, Dec. 2018.

(9) M. Tran, A. Kuwana, H. Kobayashi, "Derivation of Loop Gain and Stability Test for Multiple Feedback Low Pass Filter Using Deboo Integrator", The 8th IIAE International Conference on Industrial Application Engineering, Shimane, Japan, March, 2020.

(10) Q. Hu, L. Yang, F. Huang, "A 100–170MHz Fully-Differential Sallen-Key 6th-order Low-Pass Filter for Wideband Wireless Communication", IEEE International Conference on Integrated Circuits and Microsystems (ICICM), Chengdu, China, Sep. 2016.